Grid-Supportive Mobile Charging Stations for Decarbonization of Construction Electric Vehicles

Akın Taşcıkaraoğlu, *Senior Member, IEEE*, Muhammed A. Beyazıt, *Graduate Student Member, IEEE*, Jan Kleissl, Michael Ferry, Mohammad R. Salehizadeh, *Senior Member, IEEE*, Yuanyuan Shi, *Member, IEEE*

***Abstract*—Heavy-duty vehicles (HDVs) contribute substantially to greenhouse gas emissions, making their electrification crucial for decarbonizing the transportation and construction sectors. Transitioning construction vehicles from internal combustion engines (ICEs) to electric versions demands significant investment in charging infrastructure. Although distributing construction electric vehicle (CEV) charging across different electric vehicle (EV) charging plazas could minimize these impacts, this is often infeasible due to CEVs' poor mobility. Establishing fixed charging stations (FCSs) is costly, time-consuming, and impractical given CEVs' high power demands and transient nature of construction projects. The main objective of the study is to demonstrate the feasibility of mobile charging stations (MCSs) as a cost-effective solution for CEV charging and accelerated construction electrification, decarbonization, and air pollutant reduction. The proposed MCS-to-CEV charging solution is tested at five construction sites at University of California (UC) San Diego, which serves as an ideal host site to validate the proposed technology and benefits with very intense construction activities. The comparisons show that the following reductions are achieved: 87% less carbon emission and 96% less operating costs versus ICE-powered construction vehicles as well as 16% less energy drawn from the grid and 35% less charging time (including traveling, waiting and charging) versus FCSs.**

***Index Terms*—Carbon emissions reduction, charging cost minimization, construction electric vehicles, mobile charging stations.**

This work is supported by California Energy Commission - Energy Research Development Division under the award under GFO-23-306. The work of A. Taşcıkaraoğlu is supported by The Scientific and Technological Research Council of Türkiye (TÜBİTAK) 2219 International Postdoctoral Research Fellowship Program, and also by the Turkish Academy of Sciences through the Distinguished Young Scientist Award Program.

A. Taşcıkaraoğlu and M. A. Beyazıt are with Electrical and Electronics Engineering Department, Muğla Sıtkı Koçman University, Muğla, 48000 Türkiye. A. Taşcıkaraoğlu is also with Electrical and Computer Engineering Department, University of California San Diego, California, 92093 USA (e-mail: akintascikaraoglu@mu.edu.tr, muhammedbeyazit@mu.edu.tr).

J. Kleissl and M. Ferry are with the Center for Energy Research, University of California San Diego, California, 92093 USA (e-mail: jkleissl@ucsd.edu, mdferry@ucsd.edu).

M. R. Salehizadeh is with the Institute of Cleaner Production Technology, Pukyong National University, Busan, 48513, Republic of Korea (e-mail: salehizadeh@pknu.ac.kr).

Y. Shi is with Electrical and Computer Engineering Department, University of California San Diego, California, 92093 USA (e-mail: yyshi@ucsd.edu).

NOMENCLATURE

The indices, sets, parameters, and variables used throughout the paper are outlined below.

A. Indices

e	Index of construction electric vehicles (CEVs)
i, j	Index of nodes
m	Index of mobile charging stations (MCSs)
t, tt	Index of time intervals

B. Sets

M	Set of MCSs, $m \in M$
T	Set of time intervals, $t \in T$
N	Set of nodes, $i, j \in N$
N_0	Set of grid connection nodes
N'	Set of construction facility nodes
S	Set of paths, $(i, j) \in S$

C. Parameters

$A_{i,e}$	Binary parameter; 1 if CEV e located at construction node i, else 0
$C^{\text{MCS,plug}}$	Number of plugs on MCSs
CH^{MCS}	Charging power rate of MCSs
CH_e^{CEV}	Charging power rate of CEV e
DCH^{MCS}	Discharging power rate of MCSs
$DCH^{\text{MCS,plug}}$	Discharging power rate of each plug mounted on MCSs
$D_{i,j}$	Distance matrix of nodes (i, j) (mile)
k^{way}	Energy consumed per mile during the travel of MCS (kWh/mile)
M	A large positive number
$R_{i,e,t}^{\text{work}}$	Power consumption of CEV e in time t to accomplish work at construction node i
$\text{SOE}_e^{\text{CEV,ini}}$	Initial state-of-energy (SOE) of CEV e (kWh)
$\text{SOE}_e^{\text{CEV,max}}$	Maximum SOE of CEV e (kWh)
$\text{SOE}_e^{\text{CEV,min}}$	Minimum SOE of CEV e (kWh)
$\text{SOE}^{\text{MCS,ini}}$	Initial SOE of MCS's battery (kWh)
$\text{SOE}^{\text{MCS,max}}$	Maximum SOE of MCS's battery (kWh)
$\text{SOE}^{\text{MCS,min}}$	Minimum SOE of MCS's battery (kWh)
t^0	Initial time interval
t^{end}	Last time interval
$\tau_{i,j}^{\text{way}}$	Time spent traveling from node i to j

$\lambda_t^{\text{buy,elec}}$ Wholesale energy purchase price ($/kWh)
λ_t^{CO2} CO_2 emission price ($/kWh)
ρ^{miss} Penalty cost for missed work ($/kW)
$\eta^{\text{ch/dch}}$ Charging/discharging efficiency of the MCS
ΔT Time interval

D. Variables

$L_{m,i,j,t}^{\text{way}}$ Energy consumed by MCS m for travel between i to j in time interval t (kWh)
$\mathbb{L}_{m,t}^{\text{way,tot}}$ Energy consumed by MCS m for travel in time interval t (kWh)
$P_{m,i,t}^{\text{ch,MCS}}$ Charging power of MCS m at node i in time interval t (kW)
$P_{m,i,t}^{\text{dch,MCS}}$ Discharging power of MCS m at node i in time interval t (kW)
$P_{m,t}^{\text{ch,tot}}$ Total charging power of MCS m in time interval t (kW)
$P_{m,t}^{\text{dch,tot}}$ Total discharging power of MCS m in time interval t (kW)
$P_{m,i,e,t}^{\text{MCS}\rightarrow\text{CEV}}$ Power transferred from MCS m to CEV e in time interval t (kW)
$P_{i,e,t}^{missed,work}$ Power corresponding to the missed work for CEV e at construction node i in time interval t (kW)
$P_{i,e,t}^{\text{work}}$ Power consumed by CEV e in time interval t to complete task at construction node i (kW)
$\text{SOE}_{e,t}^{\text{CEV}}$ SOE of CEV e in time interval t (kWh)
$\text{SOE}_{\text{m},t}^{\text{MCS}}$ SOE of MCS m in time interval t (kWh)

E. Binary Variables

$\varrho_{m,i,e,t}$ 1 if CEV e connects to MCS m in node i, in time interval t, else 0
$\gamma_{m,i,t}^{\text{arr}}$ 1 if MCS m arrives to the node i, in time interval t, else 0
$\sigma_{m,i,t}^{\text{dep}}$ 1 if MCS m departs from the node i, in time interval t, else 0
$x_{m,i,j,t}$ 1 if MCS m travels using (i,j) route in time interval t, else 0
$\mu_{i,e,t}$ 1 if any MCS charges the CEV e at node i in time interval t, else 0
$z_{m,i,t}$ 1 if MCS m connects to the node i in time interval t, else 0

I. Introduction

CONSTRUCTION equipment significantly contributes to air pollution in urban areas during activities such as site preparation and road construction. According to the California Air Resource Board (CARB), off-road diesel engines are projected to emit 95 tons per day of nitrogen oxides (NO_x) and 3.1 tons per day of particulate matter (PM) by 2030, accounting for about 11% of the state's diesel NO_x emissions and 29% of its diesel PM emissions [1]. Construction equipment annually produces about 400 metric tons of CO_2, accounting for roughly 1.1% of global emissions [2]. The construction industry is linked to the highest number of occupational cancer cases annually, with approximately 8% attributable to diesel exhaust emissions [3]. Besides, various U.S. and EU standards [4,5] define limits for the emissions produced by construction vehicles. Electrifying construction site equipment to comply with the standards and reduce health-concerning emissions is therefore vital for public health and creating cleaner construction sites, aiding global climate goals.

In response to CARB's 2014 regulations, the Clean Off-Road Equipment Voucher Incentive Project (CORE) was launched in 2020 to promote zero-emission electric vehicles (EVs) among heavy-duty vehicle (HDV) operators. By November 2022, CORE had transitioned 1,430 vehicles to electric, cutting 23,100 metric tons of CO_2 and other pollutants. Besides, prominent construction vehicle manufacturers, including Volvo, John Deere, and Hitachi, have all announced initiatives toward the electrification of construction vehicles [6,7]. However, the shift to construction electric vehicles (CEVs) demands significant investments in charging infrastructure. The Electric Vehicle Charging Infrastructure Assessment - AB 2127 report underscores the need for approximately 1 million EV chargers by 2030 to support an anticipated fleet of 7 million EVs, including chargers for 157,000 medium and HDVs. Moreover, the high charging power required by CEVs, which can potentially reach up to 1 MW for a single charger [8], intensifies peak demand, necessitating costly distribution grid upgrades. Given these obstacles, coupled with the inherently poor mobility of construction vehicles, relying on existing charging infrastructure proves insufficient. This situation underscores the urgent need for innovative charging solutions tailored to CEVs.

Several studies in the literature have explored heavy-duty electric vehicle (HDEV) charging strategies. Some studies suggest redistributing HDEV charging across multiple fixed charging stations (FCSs) to minimize waiting times and/or grid impacts. A mathematical model for the HDEV routing problem is presented in [9] to reduce the transportation costs and waiting times at FCSs. An optimization approach is proposed in [10] to reduce the carbon emissions due to operation of a number of HDEVs. The study demonstrates that different emission factors from charging stations connected to different local electric grids have an important effect on the decarbonization of HDV electrification. The results presented in these two studies show that they might be effective for HDEVs; however, the poor mobility of CEVs makes these strategies impractical for their charging. Alternatively, charging all CEVs at the nearest FCS to reduce travel time results in excessive peak demand, straining power distribution systems and necessitating costly grid upgrades.

Some businesses have installed their own charging facilities for HDEVs to address peak demand issues. For instance, a data-driven strategy is introduced in [11] to minimize the overall cost of HDEV operation in a microgrid at the

University of California Riverside, by also considering the necessary investments for charging infrastructures. The findings show that considerable energy savings might be achieved for HDEVs with fixed travel schedules. Equipping FCSs with renewable energy sources (RESs) is suggested as another potential solution to reduce the grid impacts and operational costs [12]. The authors of [13] propose to use distributed and centralized RESs at FCSs for charging HDEVs with reduced cost of power purchased from grid. However, several costs, such as transmission expansion costs, are ignored in this study, which leads to underestimation of the total costs. In the case of CEVs, the chargers to be deployed for CEVs during construction will require significant investment and lengthy new installation permits. Also, it is difficult to carve out a dedicated space for chargers at construction sites as often every square foot of the construction site undergoes construction at some point.

Battery swapping has been considered as a fast and grid-independent solution for HDEVs in the literature. The authors of [14] carry out an economic evaluation of battery swapping stations for HDEVs charging and propose a scheduling method based on the fluctuations in swap demand to reduce operational costs. The feasibility of battery swapping for HDEVs is investigated in [15] and it is shown that this option might be profitable if the battery swapping price is below a certain value. While battery swapping presents a potential solution, only a handful of EV brands offer models compatible with this solution and none are available for CEVs [16]. In summary, existing strategies do not adequately address the unique challenges of CEV charging—strict schedules, substantial grid impact, and need for mobility and rapid setup—underscoring the need for innovative charging solutions.

As a solution, this study proposes to use an integrated mobile charging station (MCS) solution for CEV charging. MCSs reduce carbon emissions and criteria air pollution, lower operational costs, and achieve grid benefits including reduced peak demand, increased utilization of the existing charging infrastructure and renewable self-consumption. MCSs are portable charging units, requiring no fixed installations and are designed for frequent relocation via pickup truck to meet diverse charging demands [17,18]. We aim to create a comprehensive optimization framework to meet the charging demand of different types of CEVs such as excavators, wheel loaders, and compactors using MCSs, with the goal of minimizing the electricity costs and carbon emission of charging, while satisfying the construction schedule requirement, and the physical constraints of CEVs, MCSs, charging stations and the grid. Since construction activities typically end by 4 pm, using MCSs to charge CEVs during peak grid demand hours (4-10 pm) and recharging them during off-peak times (noon or post-10 pm) has the potential to significantly decrease peak period energy demand compared to charging all equipment simultaneously at FCSs during peak hours. MCSs also save charging time considering the travel distance between the construction site and FCSs.

The main contributions of this study are outlined below:

- An integrated MCS-to-CEV charging optimization framework is developed for the first time in the literature to identify the best locations, timings, and rates for CEV charging and MCS recharging.
- The proposed framework optimizes carbon emissions, MCS charging costs, and CEV charging times for the first time, while adhering to construction schedules and the capacities of MCSs, CEVs, and grid.
- The MCS-to-CEV system is tested at five UC San Diego construction sites, evaluating its advantages over internal combustion engine (ICE)-powered vehicles in carbon emissions and operating costs, and over FCSs in peak power demand and charging time.

The remainder of the paper is structured as follows: Section II outlines the system architecture and problem formulation of the proposed framework. Section III presents the case studies and simulation results. The feasibility of MCSs for CEV charging is analyzed in Section IV. Lastly, the conclusions are summarized in the final section.

II. METHODOLOGY

A. System Description

To meet the CEV charging demands in a specific area, a CEV charging framework consisting of MCSs, depots for MCS charging, and construction sites is proposed in this study, as depicted in Fig. 1. A system operator is assumed to be the owner of the MCSs in the considered area, similar to the approaches adopted in [19,20], and the CEVs in this area are charged through MCSs towed by electric pickups. Each MCS supports charging three CEVs at a time, with the ability to sequentially charge additional vehicles.

The MCS-to-CEV charging optimization determines the optimal locations, timings, and rates for charging CEVs and recharging MCSs to minimize carbon emissions, reduce MCS charging costs, shorten CEV charging times, and increase RES utilization, taking into account the construction schedule, and the power/energy capacities of MCSs, CEVs, and grid, as shown in Fig. 2.

B. Mathematical Model of the EV Charging Framework

The objective function defined for the proposed optimization problem and the mathematical model of MCSs are described in the following subsections.

1) Objective Function

The objective of the proposed framework is to minimize the total carbon emissions, λ_t^{CO2}, and electricity costs, $\lambda_t^{\mathrm{buy,elec}}$, associated with MCS charging as outlined in (1). $P_{i,e,t}^{missed,work}$ represents the missed work for each CEV at construction node i due to recharging activities, while ρ^{miss} is a large penalty constant introduced to allow missed works only when absolutely necessary. Essentially, the framework seeks to identify the optimal intersection of minimal carbon emissions and electricity costs for MCS charging, while adhering to the working schedules as closely as possible.

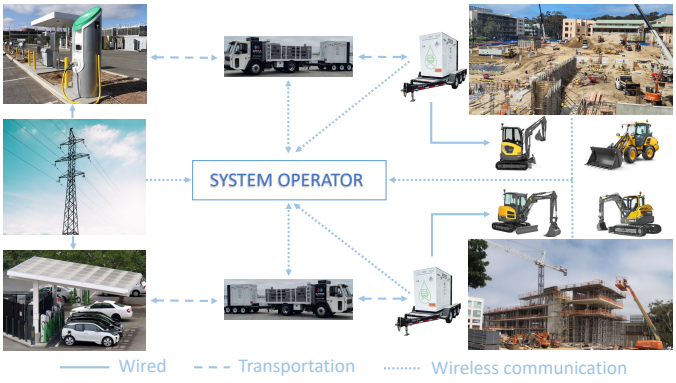

Fig. 1. Conceptual overview of the proposed MCS-to-CEV system.

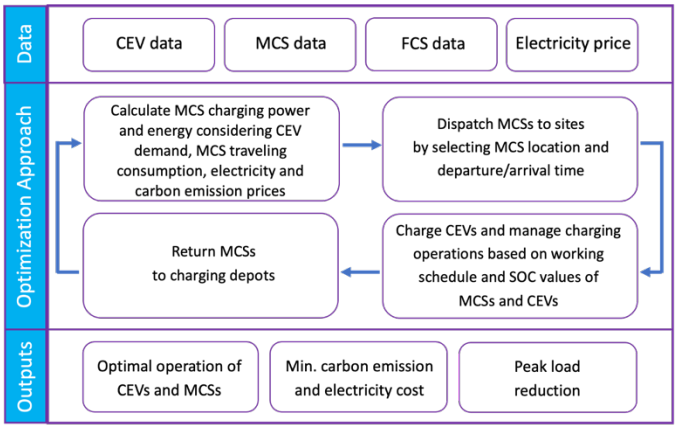

Fig. 2. Schematic representation of the proposed optimization algorithm.

$$min \sum_{m,t} P_{m,t}^{\mathrm{ch,tot}} \cdot (\lambda_t^{\mathrm{CO2}} + \lambda_t^{\mathrm{buy,elec}}) \cdot \Delta T + \sum_{i,e,t} P_{i,e,t}^{missed,work} \cdot \rho^{miss} \quad (1)$$

2) Constraints

The constraints for charging and discharging power are provided in (2) – (13). Equation (2) computes the total charging power, $P_{m,t}^{\mathrm{ch,tot}}$, as the sum of the charging power of MCS m, $P_{m,i,t}^{\mathrm{ch,MCS}}$, over $i \in N^o$. Similarly, the total discharging power, $P_{m,t}^{\mathrm{dch,tot}}$, is determined in (3) as the sum of discharging power, $P_{m,i,t}^{\mathrm{dch,MCS}}$, of MCS m over $i \in N'$. The total discharged power of MCS m at construction node i is equal to the sum of the power injected to each CEV, $P_{m,i,e,t}^{\mathrm{MCS\to CEV}}$, over e in time t, as indicated in (4). Constraint (5) prevents charging of MCSs out of the depot nodes, while constraint (6) allows discharging of MCSs only when they are connected to the construction nodes.

$$P_{m,t}^{\mathrm{ch,tot}} = \sum_{i \in N^o} P_{m,i,t}^{\mathrm{ch,MCS}}, \forall m \in M, \forall t \in T \quad (2)$$

$$P_{m,t}^{\mathrm{dch,tot}} = \sum_{i \in N'} P_{m,i,t}^{\mathrm{dch,MCS}}, \forall m \in M, \forall t \in T \quad (3)$$

$$P_{m,i,t}^{\mathrm{dch,MCS}} = \sum_{e \in E} P_{m,i,e,t}^{\mathrm{MCS\to CEV}}, \forall m \in M, \forall i \in N', \forall t \in T \quad (4)$$

$$P_{m,i,t}^{\mathrm{ch,MCS}} = 0, \forall m \in M, \forall i \in N', \forall t \in T \quad (5)$$

$$P_{m,i,t}^{\mathrm{dch,MCS}} = 0, \forall m \in M, \forall i \in N^0, \forall t \in T \quad (6)$$

$$P_{m,i,t}^{\mathrm{ch,MCS}} \le CH^{\mathrm{MCS}} \cdot z_{m,i,t}, z_{m,i,t} \in \{0,1\}, \forall m \in M, \forall i \in N^0, \forall t \in T \quad (7)$$

$$P_{m,i,t}^{\mathrm{dch,MCS}} \le DCH^{\mathrm{MCS}} \cdot z_{m,i,t}, z_{m,i,t} \in \{0,1\}, \forall m \in M, \forall i \in N', \forall t \in T \quad (8)$$

$$P_{m,i,e,t}^{\mathrm{MCS\to CEV}} \le DCH^{\mathrm{MCS,plug}} \cdot \varrho_{m,i,e,t}, \varrho_{m,i,e,t} \in \{0,1\}, \forall m \in M, \forall i \in N', \forall e \in E, \forall t \in T \quad (9)$$

$$\sum_{m \in M} P_{m,i,e,t}^{\mathrm{MCS\to CEV}} \le CH_e^{\mathrm{CEV}} \cdot \mu_{i,e,t}, \mu_{i,e,t} \in \{0,1\}, \forall i \in N', \forall e \in E, \forall t \in T \quad (10)$$

$$P_{i,e,t}^{\mathrm{work}} \le M \cdot (1 - \mu_{i,e,t}), \mu_{i,e,t} \in \{0,1\}, \forall i \in N', \forall e \in E, \forall t \in T \quad (11)$$

$$P_{i,e,t}^{\mathrm{work}} \le R_{i,e,t}^{\mathrm{work}}, \forall i \in N', \forall e \in E, \forall t \in T \quad (12)$$

$$P_{i,e,t}^{missed,work} = R_{i,e,t}^{\mathrm{work}} - P_{i,e,t}^{\mathrm{work}}, \forall i \in N', \forall e \in E, \forall t \in T \quad (13)$$

In (7), the charging power of MCSs, $P_{m,i,t}^{\mathrm{ch,MCS}}$, is restricted by the charging power rate, CH^{MCS}, while (8) limits the discharging power of MCS m to the total discharging power rate of the plugs mounted on the MCS, DCH^{MCS}. In constraints (7) and (8), the binary variable $z_{m,i,t}$ checks the connection status of MCS m in time t to start a charging/discharging session. Constraint (9) ensures that the discharging powers of the plugs mounted on MCS m are limited by $DCH^{\mathrm{MCS,plug}}$, the discharging power of the MCS plug, to charge CEV e at construction node i in time t. Moreover, the binary variable $\varrho_{m,i,e,t}$ takes a value of 1 when CEV e connects to MCS m in time t to initiate a charging session; otherwise, it takes a value of 0. The charging powers of CEVs are also limited by the charging power rate of each CEV, CH_e^{CEV}, as specified in (10).

The binary variable $\mu_{i,e,t}$ in (10) and (11) prevents CEV e from charging and discharging simultaneously. Here, $P_{i,e,t}^{\mathrm{work}}$ represents the power consumption of CEV e to perform work at construction node i in time t. Constraint (12) ensures that $P_{i,e,t}^{\mathrm{work}}$ is less than or equal to the power required to accomplish work at construction node i in time t, $R_{i,e,t}^{\mathrm{work}}$. Equation (13) calculates the missed work for each CEV e at construction node i in time t, based on the difference between the scheduled work and the performed work.

$$L_{m,i,j,t}^{\mathrm{way}} = k^{\mathrm{way}} \cdot D_{i,j} \cdot x_{m,i,j,t}, x_{m,i,j,t} \in \{0,1\}, \forall m \in M, \forall (i,j) \in S, \forall t \in T \quad (14)$$

$$\mathbb{L}_{m,t}^{\mathrm{way,tot}} = \sum_{(i,j) \in S} L_{m,i,j,t}^{\mathrm{way}}, \forall m \in M, \forall t \in T \quad (15)$$

$$\mathrm{SOE}_{m,t}^{\mathrm{MCS}} = \mathrm{SOE}_{m,t-1}^{\mathrm{MCS}} + (P_{m,t}^{\mathrm{ch,tot}} \cdot \Delta T \cdot \eta^{\mathrm{ch}}) - (P_{m,t}^{\mathrm{dch,tot}} \cdot \Delta T)/\eta^{\mathrm{dch}} - \mathbb{L}_{m,t}^{\mathrm{way}}, \forall m \in M, \quad \text{if } t \neq t^0 \tag{16}$$

$$\mathrm{SOE}^{\mathrm{MCS,min}} \leq \mathrm{SOE}_{m,t}^{\mathrm{MCS}} \leq \mathrm{SOE}^{\mathrm{MCS,max}}, \forall m \in M, \forall t \in T \tag{17}$$

$$\mathrm{SOE}_{m,t}^{\mathrm{MCS}} = \mathrm{SOE}^{\mathrm{MCS,ini}}, \forall m \in M, \text{if } t = t^0 \vee t^{\mathrm{end}} \tag{18}$$

$$\mathrm{SOE}_{e,t}^{\mathrm{CEV}} = \mathrm{SOE}_{e,t-1}^{\mathrm{CEV}} + \sum_{m \epsilon M, i \epsilon N'} (P_{m,i,e,t}^{\mathrm{MCS}\rightarrow\mathrm{CEV}} - P_{i,e,t}^{\mathrm{work}}) \cdot \Delta T, \forall e \in E, \text{if } t \neq t^0 \tag{19}$$

$$\mathrm{SOE}_{e}^{\mathrm{CEV,min}} \leq \mathrm{SOE}_{e,t}^{\mathrm{CEV}} \leq \mathrm{SOE}_{e}^{\mathrm{CEV,max}}, \forall e \in E, \forall t \in T \tag{20}$$

$$\mathrm{SOE}_{e,t}^{\mathrm{CEV}} = \mathrm{SOE}_{e}^{\mathrm{CEV,ini}}, \forall e \in E, \text{if } t = t^0 \vee t^{\mathrm{end}} \tag{21}$$

The energy consumption constraints of MCSs and CEVs are demonstrated in (14) – (21). Equations (14) and (15) calculate the energy consumption on the way for each MCS, $L_{m,i,j,t}^{\mathrm{way}}$, and the total energy used, $\mathbb{L}_{m,t}^{\mathrm{way,tot}}$, respectively. Here k^{way} represents the energy consumption of MCSs per mile, $D_{i,j}$ represents the distance between nodes in miles, and the binary variable $x_{m,i,j,t}$ is a decision variable that determines the path selection between $(i,j) \in S$. Equation (16) relates each MCS's state of energy (SOE) to the stored energy at the previous step, charging, discharging, and road energy use. Equation (17) sets minimum and maximum energy limits of MCSs ($\mathrm{SOE}^{\mathrm{MCS,min}}$ and $\mathrm{SOE}^{\mathrm{MCS,max}}$) to prevent overcharge and deep discharge. Constraint (18) ensures that the SOE of MCSs is equal to the initial value, $\mathrm{SOE}^{\mathrm{MCS,ini}}$, at the beginning of the test day, and returns to same value at the end of the test day. For CEVs, the SOE is calculated in (19) based on the stored energy from the previous step, where the charging energy comes from MCSs and energy is discharged to accomplish work at construction node i. The minimum ($\mathrm{SOE}_{e}^{\mathrm{CEV,min}}$) and maximum ($\mathrm{SOE}_{e}^{\mathrm{CEV,max}}$) SOE limits for each CEV are determined in (20), while the initial SOE values are specified in (21) to ensure that SOE of each CEV equals to $\mathrm{SOE}_{e}^{\mathrm{CEV,ini}}$ at both the beginning and end of the test day.

$$\sum_{e \in E} \varrho_{m,i,e,t} \leq C^{\mathrm{MCS,plug}}, \varrho_{m,i,e,t} \in \{0,1\}, \forall m \in M, \forall i \in N', \forall t \in T \tag{22}$$

$$\varrho_{m,i,e,t} \leq A_{i,e}, \varrho_{m,i,e,t} \in \{0,1\}, \forall m \in M, \forall i \in N, \forall e \in E, \forall t \in T \tag{23}$$

$$\sum_{i \in N, t \in T} x_{m,i,j,t} = \sum_{i \in N, t \in T} x_{m,j,i,t}, x_{m,i,j,t} \in \{0,1\}, \forall j \in N, \forall (i,j) \in S \tag{24}$$

$$\gamma_{m,i,t}^{\mathrm{arr}} - \sigma_{m,i,t}^{\mathrm{dep}} = z_{m,i,t} - z_{m,i,t-1}, \gamma_{m,i,t}^{\mathrm{arr}} \in \{0,1\}, \sigma_{m,i,t}^{\mathrm{dep}} \in \{0,1\}, z_{m,i,t} \in \{0,1\}, \forall m \in M, \forall i \in N', \text{if } t \neq t^0 \tag{25}$$

The spatial movement and connection status of the MCSs are expressed in (22) - (34). Equation (22) indicates that the number of CEVs connected to MCS m at construction node i is limited by the number of available plugs on MCS m in time t. Constraint (23) ensures that the binary variable $\varrho_{m,i,e,t}$ can take a value of 1, only if the binary parameter $A_{i,e}$, which represents the location of CEV e, is equal to 1. Therefore, MCS m can only charge CEV e at the construction node i where CEV e is located. The binary variables $z_{m,i,t}$, $\gamma_{m,i,t}^{\mathrm{arr}}$, $\sigma_{m,i,t}^{\mathrm{dep}}$, and $x_{m,i,j,t}$ define spatio-temporal connections, controlling MCS movements between nodes based on scheduled working times of CEVs. The binary variable $x_{m,j,i,t}$ determines whether MCS m goes from node i to node j. Constraint (24) guarantees that the number of arrivals at and departures from each node is equal for MCS m. The binary variable $\gamma_{m,i,t}^{\mathrm{arr}}$ takes a value of 1 when MCS m arrives at node i in time t. Similarly, the binary variable $\sigma_{m,i,t}^{\mathrm{dep}}$ takes a value of 1 if MCS m departs from node i during the specific time interval. Thus, the connection status of MCS m, denoted by the binary variable $z_{m,i,t}$ is derived based on the corresponding arrival and departure times, as described in (25).

$$z_{m,i,t} = 1, z_{m,i,t} \in \{0,1\}, \forall m \in M, \forall i \in N^0, \text{if } t = t^0 \tag{26}$$

$$\gamma_{m,i,t}^{\mathrm{arr}} = 0, \gamma_{m,i,t}^{\mathrm{arr}} \in \{0,1\}, \forall m \in M, \forall i \in N, \text{if } t = t^0 \tag{27}$$

$$\sigma_{m,i,t}^{\mathrm{dep}} = 0, \sigma_{m,i,t}^{\mathrm{dep}} \in \{0,1\}, \forall m \in M, \forall i \in N, \text{if } t = t^0 \tag{28}$$

$$\sum_{i \in N} z_{m,i,t} \leq 1, z_{m,i,t} \in \{0,1\}, \forall m \in M, \forall t \in T \tag{29}$$

$$x_{m,i,j,tt} \leq \sigma_{m,i,t}^{\mathrm{dep}}, x_{m,i,j,tt} \in \{0,1\}, \forall m \in M, \forall (i,j) \in S, \{\forall tt \geq t + \mathrm{T}_{i,j}^{\mathrm{way}}\} \tag{30}$$

$$\gamma_{m,j,t}^{\mathrm{arr}} = \sum_{i \in N} x_{m,i,j,t}, \gamma_{m,j,t}^{\mathrm{arr}} \in \{0,1\}, \forall m \in M, \forall (i,j) \in S, \forall t \in T \tag{31}$$

$$\gamma_{m,i,t}^{\mathrm{arr}} + \sigma_{m,i,t}^{\mathrm{dep}} \leq 1, \gamma_{m,i,t}^{\mathrm{arr}} \in \{0,1\}, \sigma_{m,i,t}^{\mathrm{dep}} \in \{0,1\}, \forall m \in M, \forall i \in N, \forall t \in T \tag{32}$$

$$\sum_{t \in T} \gamma_{m,j,t}^{\mathrm{arr}} \leq 1, \gamma_{m,j,t}^{\mathrm{arr}} \in \{0,1\}, \forall m \in M, \forall i \in N' \tag{33}$$

$$\sum_{t \in T} \sigma_{m,i,t}^{\mathrm{dep}} \leq 1, \sigma_{m,i,t}^{\mathrm{dep}} \in \{0,1\}, \forall m \in M, \forall i \in N' \tag{34}$$

Constraints (26) – (28) ensure that the MCSs are initially connected to a depot node at the beginning of the test day and can begin moving after the initial time interval t^0. Constraint (29) avoids MCSs from visiting multiple nodes in the same time interval. Constraint (30) specifies that MCS m must leave node i in time t to arrive at node j in time tt. When the binary variable $x_{m,i,j,t}$ equals 1, indicating that MCS m reaches node j in time t, the condition outlined in (31) must hold. To avoid any overlap where an MCS both arrives and departs from the same node within the same time, constraint (32) is enforced. Equations (33) and (34) limit MCS m to a single visit to each

construction node per day, reducing unnecessary traffic and mitigating congestion issues, especially in constrained environments, such as university campuses or narrow urban streets.

III. Test and Results

A. Simulation Setup

Five demonstration sites located at the University of California (UC) San Diego are selected for the simulation studies. UC San Diego serves as a unique and ideal site to validate the proposed MCS-CEV solution for construction electrification as there are numerous planned construction activities. At the identified construction sites, two of which are shown in Fig. 3 (a), the proposed MCS-to-CEV solution is tested with 20 CEVs with 20-230 kW of power performing regular construction activities and 4 MCSs over one day. The MCSs are designed to be towed by a truck multiple times daily and can be recharged at standard Level II EVSE AC chargers and Level III DC fast chargers (DCFCs), but only DCFC are considered here due to the increased speed of recharging. Convenient recharging locations with DCFCs for the MCSs are marked with red triangles in Fig. 3 (b) at the East Campus Utility Plant and the P707 parking lot.

B. Input Data

This study investigates the decarbonization of CEVs over a single day, starting at 07:00 h on November 5, 2024, and ending at 06:45 h the following day. The initial SOE level of the CEVs is assumed to be 100%, while MCSs are initialized at 50% of their battery capacity. To extend the battery life, the minimum SOE levels for both CEVs and MCSs are constrained to 20%. Each MCS is equipped with three charging plugs, enabling the simultaneous charging of multiple CEVs within the same time interval. The specifications of the MCSs and CEVs used in the simulations are detailed in Table 1 and Table 2, respectively. The working hours and time-matched power requirements for completing tasks at construction sites are shown in Fig. 4.

The working hours are set as 07:00–12:00 and 13:00–16:00, in compliance with city noise ordinances and daily working hour limits for workers. Different types and numbers of CEVs are used in the five construction areas. To account for differing operation schedules, it is assumed that two construction sites, Site-1 and Site-4, operate for half a day, while the remaining sites operate for a full day. The efficiencies of ICE-powered construction vehicles and CEVs are assumed to be 30% and 90%, respectively [21,22]. The locational marginal electricity price and carbon emission data obtained from the California Independent System Operator (CAISO) for the considered day are given in Fig. 5. We assume that MCS operator purchases energy in the wholesale market as is the case for UC San Diego. At other sites, higher retail energy rates and demand charges would have to be considered, which would increase energy costs roughly by a factor of 10. Carbon emission prices for the entire day were derived using the social cost of carbon, estimated by the U.S. government at $50 per metric ton [23].

(a) (b)

Fig. 3. (a) Two of the five proposed UC San Diego demonstration sites: Triton center (top) and Ridge Walk North Living and Learning Neighborhood (bottom), (b) Recharging locations for MCSs with DC fast chargers.

TABLE I
Technical specifications of the MCS [24-26].

SOE [kWh]	Charging Efficiency [%]	Charging rate [kW]	Road Energy consumption [kWh/mile]
250	95	125	0.5

TABLE II
Technical specifications of the CEVs [6].

	Excavator	Mini excavator	Wheel loader	Compactor
Quantity [Unit]	2	8	5	5
Power [kW]	230.0	25.0	20.0	25.0
Energy [kWh]	264.0	20.0	40.0	20.0
Max. Speed [mph]	3.5	2.8	12.4	6.4
Consumption on road [kWh/mile]	2.0	0.6	0.8	0.6
Total energy consumed [kWh/day]	235.7	120.8	93.6	96.7

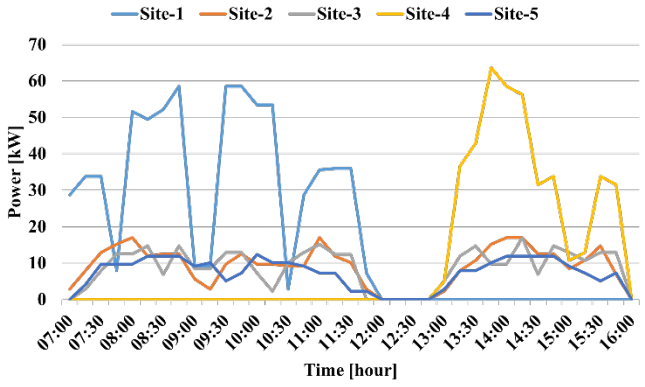

Fig. 4. Total power requirements for completing tasks at the five construction sites for the considered day.

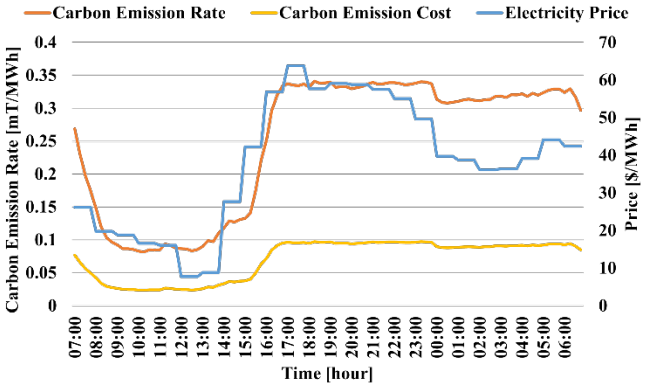

Fig. 5. Daily electricity price and carbon emission values [27].

C. Simulation and Results

To evaluate the benefits, the MCS-to-CEV system is compared with ICE-powered vehicles and FCSs in terms of several metrics, including carbon emissions, air pollutant emissions, operating energy costs, missed work, and peak-hour charging load reduction. The analysis is conducted through the following case studies:

- **Base Case:** 20 traditional ICE-powered construction vehicles are deployed at the construction sites. CEVs and MCSs are not integrated into the system.
- **Case-1:** 20 CEVs are utilized across the construction sites, with FCSs integrated for charging. CEVs are charged immediately after completing their work (FCS).
- **Case-2:** 20 CEVs are utilized across the construction sites, with FCSs integrated for charging. CEV charging is controlled to minimize total costs associated with carbon emissions and electricity costs (FCS-V1G).
- **Case-3:** 20 CEVs are utilized across the construction sites and charged by 4 MCSs. CEV charging is controlled to minimize total costs associated with carbon emissions and electricity costs (MCS-V1G).

In the Base Case, it is assumed that fuel trucks deliver diesel and gasoline to the construction sites every other day for refueling the construction vehicles. For simplicity, the fuel consumption of the fuel delivery trucks is excluded from the analysis in this study. In Case-1 and Case-2, CEVs are used instead of ICE-powered construction vehicles, with their recharging needs supplied by FCSs that rely on grid power throughout the day. In Case-1, to reflect real-world conditions, CEVs are primarily charged immediately by FCSs after completing their tasks to prepare for the following day's operations. In contrast, in the FCS-V1G case, CEVs charging is controlled after completing their tasks, aiming to minimize the total carbon emissions and electricity costs.

In both Case-1 and Case-2, CEVs must travel from construction sites to FCSs for recharging based on their working schedules and residual SOE. This travel requirement results in missed work within the work schedule. However, in Case-3, the CEV charging needs are met by MCSs located directly at the construction sites. These MCSs travel between the construction sites and depots, enabling on-site charging and eliminating work schedule disruptions. Although missed work does not occur under the considered work schedule for the MCS-V1G case, it may still occur in scenarios with tight and prolonged working schedules, as CEVs cannot operate while charging.

Figure 6 illustrates the charging power of CEVs for Cases 1-3. In Case-1 and Case-2, CEVs are typically charged during specific time windows, such as 1-hour lunch breaks, evenings, or nighttime, to minimize delays in the work schedule. Lunch break charging also contributes to cost minimization by aligning with low-carbon emission and low-price periods. Case-1 employs immediate charging after task completion, while Case-2 employs an optimized charging strategy. In contrast, Case-3 allows for continuous and distributed charging throughout the day, as MCSs enable CEVs to recharge on-site without causing missed work in the schedule. This approach allows CEVs to charge individually as needed, ensuring they can resume their tasks immediately after charging.

As shown in Fig. 7, the power consumption of the CEVs is consistent across all the cases except for missed work in the schedule observed in Case-1 and Case-2. These missed works result in 3.9% of the scheduled work remaining unaccomplished in both cases. The total SOE variation of the CEVs, which depends on the charging/discharging power and road energy consumption, is presented in Fig. 8. The CEVs begin and complete their tasks with fully charged batteries, amounting to a total of 988 kWh for all CEVs, as shown in Fig. 8. During the day, the charging and discharging behaviors of the CEVs are similar for Case-1 and Case-2; however, they diverge in the evening due to differences in their charging schedules. In contrast, the SOE variation of the CEVs in Case-3 differs significantly, as the MCSs charge the CEVs on-site based on their current SOE values and subsequent work schedules.

Figure 9 illustrates the energy consumption on the road for Case-1, Case-2, and Case-3, calculated using the energy consumption per mile for CEVs and MCSs as given in Table 1 and Table 2. The total energy consumption of the CEVs is identical in Case-1 and Case-2, as they require the same amount of energy to complete the construction site tasks. However, the total energy consumption on the road decreases by 81% in Case-3 due to the smaller number of MCSs compared to CEVs and their smaller unit energy consumption. As a result, in Case-3, the total power drawn from the grid is reduced by 16% compared to Case-1 and Case-2.

Figure 10 shows the total charging/discharging power and individual SOE variation of the MCSs. Each MCS has a battery capacity of 250 kWh and begins the day with 50% battery capacity. The optimization algorithm identifies the lunch break as the most suitable time for recharging MCSs to minimize carbon emissions and electricity costs. Since the discharging power of MCSs corresponds to the charging requirements of CEVs, the discharging power of MCSs matches the charging power of CEVs in Case-3. Finally, the SOE of each MCS varies depending on its charging/discharging power and road energy consumption.

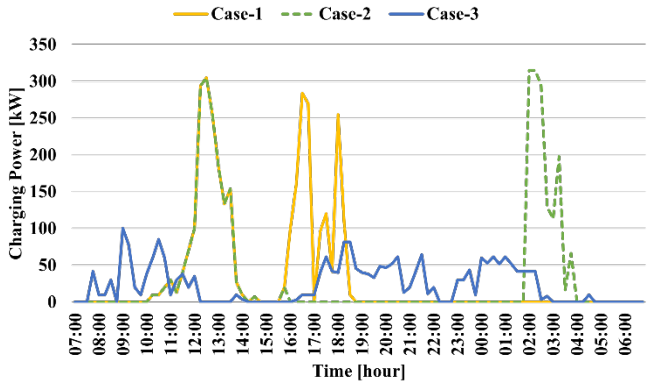

Fig. 6. Charging power of CEVs for Case-1, Case-2 and Case-3.

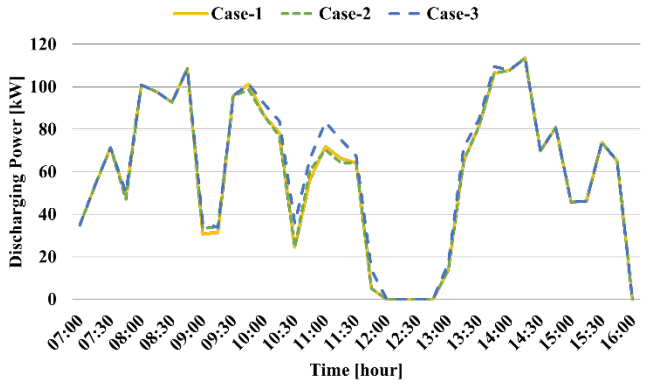

Fig. 7. Power consumption of CEVs for Case-1, Case-2 and Case-3.

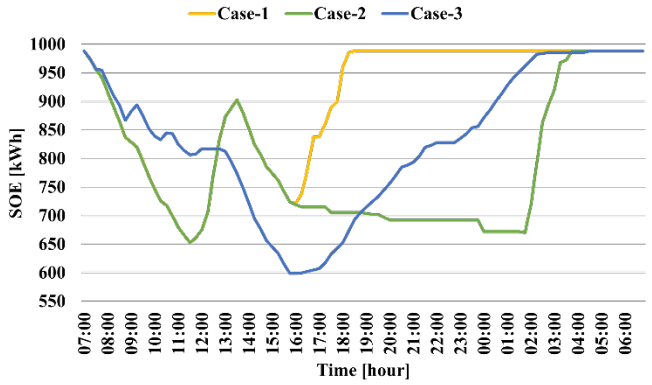

Fig. 8. SOE of all CEVs combined for Case-1, Case-2 and Case-3.

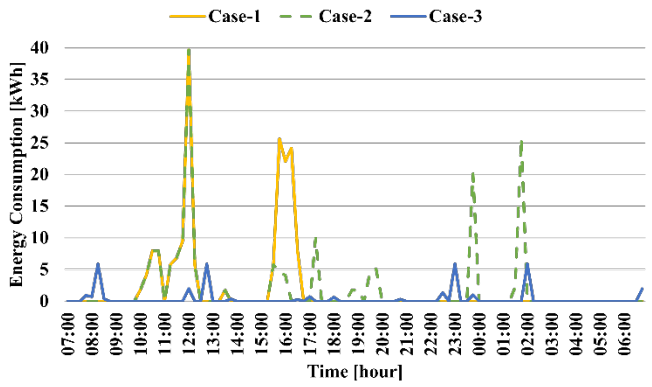

Fig. 9. Total energy consumption on the road for Case-1, Case-2 and Case-3.

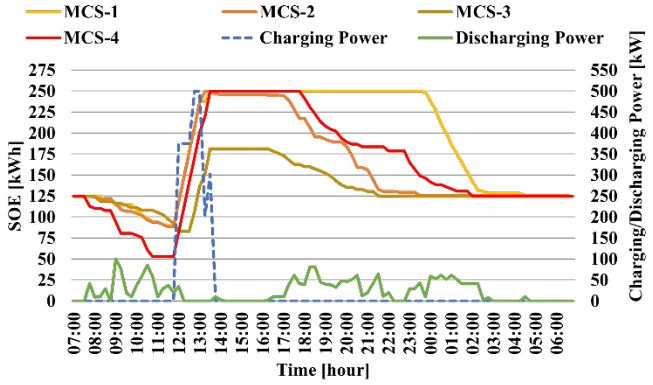

Fig. 10. Charging/discharging power and SOE variations of each MCS for Case-3.

A detailed comparison of the case studies based on peak-hour charging load reduction, carbon emissions, air pollutants, operating energy costs, and missed works is presented in Table 3. In this study, it is assumed that peak loading occurs on the power grid when real-time electricity prices exceed $55 per MWh. Accordingly, the peak hours are defined as 16:00 to 22:00 h. Since ICE-powered construction vehicles operate off-grid, peak-hour charging load reduction is not applicable to the Base Case. However, in the scenario where CEVs are charged immediately after completing their tasks, peak loading occurs in the evening hours. Peak loading is completely eliminated in the FCS-V1G and MCS-V1G cases.

The total carbon emissions and air pollutants for ICE-powered vehicles were calculated using unit values of 10.19 $kgCO_2$/Gal, 0.049 kgCO/Gal and 0.045 $kgNO_x$/Gal of diesel fuel, as adopted from [28,29]. For the CEVs, carbon emissions were determined using the carbon emission rates for the selected day (Fig. 5) and the charging energy of the CEVs. Consequently, the CO_2 emissions from completing tasks at construction sites are approximately reduced by 67% in Case-1 and Case-2 compared to the Base Case. In Case-3, where MCS technology is employed, carbon emissions are further reduced by 62% compared to Case-2.

The use of ICE-powered construction vehicles results in local air pollution, which is completely eliminated with CEVs in Case-1, Case-2, and Case-3. Furthermore, implementing CEVs with immediate charging reduces the total energy costs by 85% from the Base Case to Case-1, attributed to the higher diesel prices compared to electricity. When CEVs are charged with an optimized schedule or using MCS technology, total energy costs decrease by 25% and 75%, respectively compared to Case-1. However, in real-world applications, adhering to the working schedule is often prioritized over minimizing energy costs. Notably, while energy costs decrease in Case-1 and Case-2, the average working hours per CEV decline from 4.7 to 4.5 hours per day. In contrast, the use of MCSs in Case-3 eliminates the missed work in the schedule caused by the travel requirements of CEVs to FCSs, which occurs in Case-1 and Case-2.

IV. Discussion

In this study, a small-scale implementation of the MCS technology for charging CEVs is considered. The potential

TABLE III
Comparison of refueling/charging technologies in terms of various benefits.

	Peak charging load [kW]	Carbon emission [kg CO_2/day]	Air pollutants [kg CO/day]	Air pollutants [kg NO_x/day]	Operating energy cost [$/day]	Missed work [kW/day]
ICE vehicles	-	463.2	2.2	2.0	218.3	0
FCS	1447.2	154.4	0.0	0.0	32.9	89.2
FCS-V1G	0.0	151.9	0.0	0.0	24.7	89.2
MCS-V1G	0.0	58.3	0.0	0.0	8.3	0

benefits of the MCS-to-CEV charging solution compared to existing solutions for a large-scale application and advantages for accelerating construction electrification are discussed below:

Deferral of charging infrastructure and distribution grid upgrades: In 2022, over 2,000 CEVs were operating in California, with numbers projected to reach 7,500 in ten years. To accommodate this growth and ensure convenient charging, at least 550 DC fast charging ports will be required, necessitating a grid capacity upgrade of the order of 100 MW. Through their ability to shift load to hours without grid constraints, MCSs represent a significant investment savings for grid and charging infrastructure costs, estimated to be over $150M. Compared to adding permanent CEV charging stations at construction sites with limited or constrained grid capacity, the MCS charging solution reduces peak demand and defers the need for expensive distribution grid upgrades. For example, charging 20 CEVs simultaneously with DCFCs would add a peak power load of 494 kW, constituting 2% of UC San Diego's campus peak demand [30]. In contrast, MCSs allow CEVs to be charged during peak periods without impacting the grid's peak load, as MCSs can be recharged during off-peak times. Besides, the spatio-temporal flexibility of MCSs can provide further benefits for the power grids, including increased EV charging station utilization and renewable self-consumption, and enhanced resilience.

Carbon emission reductions: By replacing 7,500 ICE-powered construction vehicles with CEVs and assuming the vehicles are charged from RESs, the CO_2 emissions are reduced by up to 150 tons daily and 30,000 tons annually, based on the values in Table III.

Peak load reduction and shifting: The proposed framework allows MCSs to charge mostly during off-peak hours. The stored energy is then used to charge CEVs throughout the day, avoiding simultaneous charging during peak periods and significantly reducing demand during peak hours. Shifting electricity consumption from peak to off-peak times helps balance grid load and enhance grid efficiency and reliability. Considering the simultaneous charging of 20 CEVs, 494 kW of power is shifted to off-peak periods. Given the expected increase in CEVs, charging 25% of an estimated 7,500 CEVs in California with MCSs would shift 45 MW to off-peak times.

Accelerating CEV adoption: MCSs can remove one of the major barriers of CEVs adoption by providing a fast and cost-effective charging solution in areas with limited power capacity, which is common for construction sites where the power infrastructure is still being planned or in need of upgrades.

Emergency power resilience: MCSs also might serve a critical role in emergency power resilience. They can function as mobile storage systems, supporting mission-critical buildings during power outages [31]. Unlike traditional backup generators that may fail under extreme conditions, MCSs provide reliable backup power. This was notably relevant when two hospitals in San Diego experienced generator failures during the power outage in 2011 [32], and another failure occurred at a Northern California Hospital during the heatwave in 2022 [33]. MCSs offer a dependable alternative for emergency backup, enhancing energy resilience.

Payback period: FCSs, especially DCFC stations, are capital-intensive and have a long payback period, which is generally over ten years. MCSs provide significant opportunities for market growth. It is anticipated that the market size for MCSs will reach $400M by 2035. Together with technological developments and economies of scale, especially on batteries and fast charging technologies, it is expected that payback period will range from 3 to 7 years [15].

Noise pollution: Construction equipment contributes to noise pollution, adversely affecting human health and well-being. Sound levels under 70 dBA are safe, but continuous exposure to levels above 85 dBA, common in construction environments, can lead to severe health issues like hypertension, cardiovascular problems, and hearing loss. Diesel-fueled equipment often exceeds these safe levels, reaching 93-112 dBA. In contrast, electric construction equipment operates at significantly lower sound levels and does not require noise-generating cooling fans.

V. Conclusions

Electrification of construction vehicles, which are an important category of heavy-duty mobile non-road diesel engines, is challenging. Regular FCSs are not always designed to accommodate their size and power requirements. Constructing specialized FCSs for these vehicles results in high costs. In this study, an integrated MCS-to-CEV charging optimization framework is proposed to determine the optimal location and time for CEV charging and MCS recharging, optimizing carbon emissions, charging costs, and charging times while respecting construction schedules and system capacities. The benefits of the proposed framework are

validated through simulation studies at five real-world construction sites at UC San Diego. The comparisons reveal an 87% reduction in carbon emissions and a 96% decrease in operating costs compared to ICE-powered construction vehicles. Besides, a 16% reduction in power drawn from the grid and a 35% decrease in total charging time are achieved compared to FCS.

The study demonstrates that the proposed MCS-centered CEV charging solution effectively shifts charging loads from peak demand periods to off-peak times or periods of high renewable energy generation, enabling peak load reduction and potentially deferring costly electrical grid upgrades. Furthermore, the solution optimizes MCS routes based on the CEV charging demands and energy level of the MCS batteries, reducing travel times and corresponding energy consumption. This study highlight the potential to pave the way for expanded adoption of the proposed integrated MCS-to-CEV solution, particularly in regions with extensive construction activities.

REFERENCES

[1] Q. Yao, S. Yoon, Y. Tan, L. Liu, J. Herner, G. Scora, R. Russell, H. Zhu, and T. Durbin, “Development of an Engine Power Binning Method for Characterizing PM2.5 and NOx Emissions for Off-Road Construction Equipment with DPF and SCR”, *Atmosphere*, vol. 13, no. 6, 975, 2022.

[2] D. Wyatt, “Electric vehicles in construction 2022-2042”, IDTechEx, 2022.

[3] International Agency for Research on Cancer (IARC) Working Group on the Evaluation of Carcinogenic Risks to Humans, “Diesel and Gasoline Engine Exhausts and Some Nitroarenes”, Lyon (FR): IARC Monographs on the Evaluation of Carcinogenic Risks to Humans, No. 105, 2013.

[4] U.S. Code, Title 42, Section 7543, "State standards," Clean Air Act, 2023. [Online]. Available: https://www.law.cornell.edu/uscode/text/42/7543

[5] European Union, Regulation (EU) 2016/1628 of the European Parliament and of the Council, "Requirements relating to gaseous and particulate pollutant emission limits and type-approval for internal combustion engines for non-road mobile machinery," Sept. 14, 2016. [Online]. Available: https://eur-lex.europa.eu

[6] Volvo Construction Equipment, "Electric Machines," [Online]. Available: https://www.volvoce.com/united-states/en-us/products/electric-machines/. [Accessed: Dec. 8, 2024].

[7] Deere & Company, "Electrification," [Online]. Available: https://about.deere.com/en-us/our-company-and-purpose/technology-and-innovation/electrification/. [Accessed: Dec. 8, 2024].

[8] A. Jenn, "Emissions of electric vehicles in California’s transition to carbon neutrality," *Appl. Energy*, vol. 339, p. 120974, 2023.

[9] A. Amiri, H. Zolfagharinia, and S. H. Amin, "A robust multi-objective routing problem for heavy-duty electric trucks with uncertain energy consumption," *Comput. Ind. Eng.*, vol. 178, p. 109108, 2023.

[10] J. Lu, R. Shan, N. Kittner, W. Hu, and N. Zhang, "Emission reductions from heavy-duty freight electrification aided by smart fleet management," *Transp. Res. Part D: Transp. Environ.*, vol. 121, p. 103846, 2023.

[11] J. Yusuf, A. J. Hasan, J. Garrido, S. Ula, and M. J. Barth, "A comparative techno-economic assessment of bidirectional heavy duty and light duty plug-in electric vehicles operation: A case study," *Sustain. Cities Soc.*, vol. 95, p. 104582, 2023.

[12] A. K. Aktar, A. Taşcıkaraoğlu, O. Erdinç, and S. Güner, "Impacts of distribution-level joint scheduling of electric vehicle battery charging and swapping stations on reliability improvement," *IEEE Trans. Ind. Appl.*, vol. 60, no. 5, p. 7844 - 7857, Sept.-Oct. 2024.

[13] A. T. Pham, L. Lovdal, T. Zhang, and M. T. Craig, "A techno-economic analysis of distributed energy resources versus wholesale electricity purchases for fueling decarbonized heavy duty vehicles," *Appl. Energy*, vol. 322, p. 119460, 2022.

[14] F. Y. Wang, Z. Chen, and Z. Hu, "Comprehensive optimization of electrical heavy-duty truck battery swap stations with a SOC-dependent charge scheduling method," *Energy*, p. 132773, 2024.

[15] Z. Wang, Y. Liu, Z. Lin, H. Hao, and S. Li, "Techno-economic comparison on charging modes of battery heavy-duty vehicles in short-haul delivery: A case study of China," *J. Cleaner Prod.*, vol. 425, p. 138920, 2023.

[16] J. Bai, T. Ding, W. Jia, C. Mu, P. Siano, and M. Shahidehpour, "Battery charging and swapping system involved in demand response for joint power and transportation networks," *IEEE Trans. Intell. Transp. Syst.*, 2024.

[17] A. K. Aktar, A. Taşcıkaraoğlu, and J. P. Catalão, "Scheduling of mobile charging stations with local renewable energy sources," *Sustain. Energy Grids Netw.*, vol. 37, p. 101257, 2024.

[18] M. A. Beyazıt and A. Taşcıkaraoğlu, "Electric vehicle charging through mobile charging station deployment in coupled distribution and transportation networks," *Sustain. Energy Grids Netw.*, vol. 35, p. 101102, 2023

[19] J. Chen and K. Strunz, "Optimal electric bus charging and battery swapping with renewable energy and frequency control ancillary service through aggregator," *IEEE Trans. Transp. Electrific.*, 2024.

[20] S. Liu, J. Yan, Y. Yan, H. Zhang, J. Zhang, Y. Liu, and S. Han, "Joint operation of mobile battery, power system, and transportation system for improving the renewable energy penetration rate," *Appl. Energy*, vol. 357, p. 122455, 2024.

[21] I. Veza, M. Z. Asy'ari, M. Idris, V. Epin, I. R. Fattah, and M. Spraggon, “Electric vehicle (EV) and driving towards sustainability: Comparison between EV, HEV, PHEV, and ICE vehicles to achieve net zero emissions by 2050 from EV,” *Alex. Eng. J.*, vol. 82, p. 459-467, 2023.

[22] S. Baweja and R. Kumar, “Efficiency Improvement of Internal Combustion Engines over Time”, Novel Internal Combustion Engine Technologies for Performance Improvement and Emission Reduction, 147-173, 2021.

[23] K. W. Cheng, Y. Bian, Y. Shi, and Y. Chen, "Carbon-aware EV charging," in *Proc. 2022 IEEE Int. Conf. Commun., Control, Comput. Technol. Smart Grids (SmartGridComm)*, pp. 186–192, Oct. 2022.

[24] Saniset Fleet, "Clean Gen J250 Mobile Battery," [Online]. Available: https://www.sanisetfleet.com/mobile-battery/cleangenj250. [Accessed: Dec. 8, 2024].

[25] U.S. Department of Energy, "Fuel Economy," [Online]. Available: https://www.fueleconomy.gov/feg/Find.do?action=sbs&id=46329. [Accessed: Dec. 8, 2024].

[26] University of California San Diego, "EV Stations," [Online]. Available: https://transportation.ucsd.edu/commute/ev-stations.html. [Accessed: Dec. 8, 2024].

[27] California Independent System Operator, "Today's Outlook," [Online]. Available: https://www.caiso.com/todays-outlook/. [Accessed: Dec. 8, 2024].

[28] UNHSIMAP, "2019 Table," [Online]. Available: https://unhsimap.org/2019table. [Accessed: Dec. 8, 2024].

[29] San Diego Gas & Electric, "Emissions Calculations," [Online]. Available:https://www.sdge.com/sites/default/files/Appendix%25204.3-A_Emissions%2520Calculations_0_0.pdf. [Accessed: Dec. 8, 2024].

[30] S. Silwal, C. Mullican, Y. A. Chen, A. Ghosh, J. Dilliott, and J. Kleissl, "Open-source multi-year power generation, consumption, and storage data in a microgrid," *J. Renew. Sustain. Energy*, vol. 13, no. 2, 2021.

[31] M. R. Salehizadeh, A. K. Erenoğlu, İ. Şengör, A. Taşcıkaraoğlu, O. Erdinç, J. Liu, and J. P. Catalão, "Preventive energy management strategy before extreme weather events by modeling EVs’ opt-in preferences," *IEEE Trans. Intell. Transp. Syst.*, vol. 25, no. 11, p. 18368-18382, Nov. 2024.

[32] San Diego Union Tribune, "Regional hospitals fully operational Friday," [Online]. Available: https://www.sandiegouniontribune.com/news/health/sdut-regional-hospitals-fully-operational-friday-2011sep09-story.html#:~:text=Hospitals%20in%20the%20San%20Diego,outage%20when%20emergency%20generators%20failed. [Accessed: Dec. 8, 2024].

[33] Fierce Healthcare, "Backup generators fail Northern California hospital during record-breaking heatwave," [Online]. Available: https://www.fiercehealthcare.com/providers/backup-generators-fail-northern-california-hospital-during-record-breaking-heatwave. [Accessed: Dec. 8, 2024]